Fabrication and Characterization of Multilayer SiO_2/Polymethacrylic Acid/Polypyrrole Composites and Hollow Polypyrrole Microspheres

Wenqin Wang, Linchao Lu, Tianyang Chen, Mian Rao

Faculty of Materials Science and Chemical Engineering, Ningbo University, Ningbo 315211, People's Republic of China

Received 11 January 2011; accepted 5 December 2011
DOI 10.1002/app.36642
Published online in Wiley Online Library (wileyonlinelibrary.com).

ABSTRACT: Methacrylic acid was polymerized on the 3-(methacryloxy)propyl trimethoxysilane-modified silica core. The carboxylic acid groups of polymethacrylic acid (PMAA) not only provide the "active-sites" for growth of the pyrrole monomers but also act as doping acids for polypyrrole (PPy). By *in situ* polymerization route, SiO_2/PMAA/PPy multilayer composites and hollow PPy microspheres with controllable shell thickness were fabricated. The morphologies, sizes, and structures of the nanocomposites were investigated in detail by transmission electron microscopy, scanning electron microscopy, Fourier-transform infrared spectra, X-ray photoelectron spectroscopy, and thermogravimetric analysis.
 J Appl Polym Sci 000: 000–000, 2012

Key words: SiO_2; polypyrrole; composite; hollow microsphere

INTRODUCTION

Recently, there is increasing interest in conducting polymer core–shell nanocomposites and hollow nanocapsules due to their wide range of application.[1] In the past decade, there are a number of strategies reported for fabrication of core–shell conducting polymer nanocomposites. Among of all strategies, template-assisted method is one of the most effective and general techniques. Since the pioneered works of Khan et al.[2,3] on the preparation of the core–shell conducting polymer nanocomposites with polystyrene (PS) latex spheres as templates, various inorganic or organic materials, such as Ag,[4–6] Au,[7] Fe_2O_3,[8] Fe_3O_4,[9] PS,[10,11] and SiO_2[12,13], etc., had been used as templates to synthesize the resulting core–shell conducting polymer composites. Hollow conducting polymer capsules could be obtained easily via removal of templates, and hollow conducting polymer spheres may provide some immediate advantages over their solid counterparts for applications in various fields due to their relatively low densities.[14] Compared to other templates, the SiO_2 reveals some advantages due to its simplicity of synthetic procedure, low cost, and ease of functionalization, etc. However, it is a chief disadvantage that the hydrophilic surface of silica is not favorable for aggregation of hydrophobic monomers (pyrrole). So some research groups had devoted much effort toward surface modification of SiO_2 using different agents, such as poly(*N*-vinylpyrolidone),[15] cetyltrimethylammonium bromide,[16] and 3-(trimethoxysilyl)propyl methacrylate (MPS).[17]

In recent articles, the template-containing acidic groups, such as suflonated-PS[18–20] was more favorable for fabrication of conducting polymer core–shell composites. Inspired by the above studies, we used the SiO_2/polymethacrylic acid (PMAA) microspheres as templates to synthesize the SiO_2/PMAA/Polypyrrole (PPy). Compared with traditional modified-surface agents, the PMAA layer not only offered "active-sites" for formation of PPy on silica but also acted as doping acids for conducting polymer.

EXPERIMENTAL

Materials

Tetraethylorthosilicate was purchased from Aldrich (Milwaukee, WI). Divinylbenzene (DVB, 80% DVB isomers) was obtained from Aldrich and washed with 5% aqueous sodium hydroxide and water and then dried over anhydrous magnesium sulfate before use. MPS was purchased from Alfa and

Additional Supporting Information may be found in the online version of this article.

Correspondence to: W. Wang (wqwang@126.com).

Contract grant sponsor: K. C. Wong Magna Fund in Ningbo University and Scientific Research Foundation of Ningbo University; contract grant number: xkl09073.

Contract grant sponsor: Research Foundation for Advanced Talents of Ningbo University; contract grant number: RCL2008003.

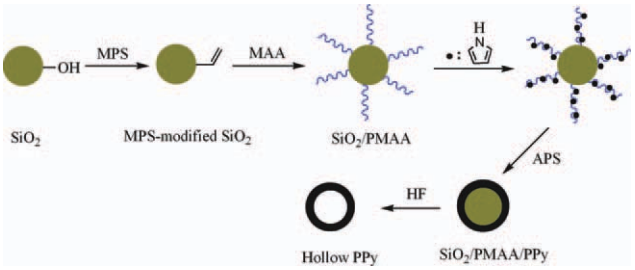

Scheme 1 Illustration of formation of SiO_2/PMAA/PPy nanocomposite and PPy hollow spheres. [Color figure can be viewed in the online issue, which is available at wileyonlinelibrary.com.]

distilled under vacuum. Acetonitrile, methacrylic acid (MAA), pyrrole, and 2,2′-azobis(isobutyronitrile) (AIBN) were obtained from Sinopharm Chemical Reagent (Shanghai, China). Acetonitrile was dried over calcium hydride and purified by distillation. MAA and pyrrole were distilled under reduced pressure before use. AIBN was recrystallized from methanol. All the other reagents were analytical reagents and used as received without any further purification.

Synthesis of SiO_2/PMAA hybrid microspheres

The MPS-modified silica nanoparticles were prepared according to the previous report.[21] The SiO_2/PMAA hybrid nanoparticles were prepared by distillation precipitation polymerization (see Supporting Information).[22] By modifying the silica using MPS, the vinyl groups were introduced on the surface of SiO_2. AIBN as an initiator, DVB as a crosslinker, MAA monomers were polymerized on the surface of SiO_2. After the polymerization, SiO_2/PMAA microspheres were separated by centrifugation and washed with ethanol. Finally, the product was dried in a vacuum oven at 50°C for 24 h.

Preparation of SiO_2/PMAA/PPy multiple nanocomposite

SiO_2/PMAA microspheres (0.1 g) were dispersed in 10 mL of deionized water by ultrasound. Different volume of pyrrole monomer was added, and the mixture solution was stirred for 2 h at room temperature. Subsequently, the oxidant ammonium persulfate (the molar ratio of oxidant to monomer was 1 : 1) was added into above solution. The reaction system was kept stirring for 12 h at room temperature. After washing by ethanol several times, the product was dried at 50°C for 24 h in vacuum oven.

Preparation of hollow spheres

The nanocomposite particles were soaked in an aqueous solution of 10 wt % hydrofluoric acid (HF) for 24 h to remove the silica cores. And then the sample was separated by centrifugation at 4000 rpm for 15 min and washed four times with deionized water. Finally, the product was dried at 50°C for 24 h in vacuum oven.

Characterization

Scanning electron microscope (SEM, S-4800) and transmission electron microscope (TEM, H-7650) were used to observe the morphologies of the nanocomposites. Fourier-transform infrared spectroscopy (FTIR 6700, Nicolet) and X-ray photoelectron spectroscope (XPS, Axis Utltradld) were used to characterize the nanocomposites. Thermogravimetric analysis (TGA) was determined with a Perkin-Elmer thermogravimetric analyzer (TG-DTA, SSC-5200) at a heating rate of 10°C min^{-1} in N_2 from room temperature up to 900°C.

RESULTS AND DISCUSSION

The fabrication of SiO_2/PMAA/PPy microspheres was described in Scheme 1. The vinyl groups were introduced to the surfaces of SiO_2 by modifying SiO_2 using MPS. Subsequently, MAA monomers were polymerized on SiO_2 to form SiO_2/PMAA microspheres. The pyrrole monomers were adsorbed on the PMAA layer and further oxidized to form SiO_2/PMAA/PPy multilayer nanocomposite. Removal of SiO_2 cores by HF, hollow PPy microspheres were obtained.

Thermogravimetric Analysis

The TG results of the products in nitrogen are shown in Figure 1. The TGA curve of SiO_2/PMAA microspheres shows a three-step weight loss. The

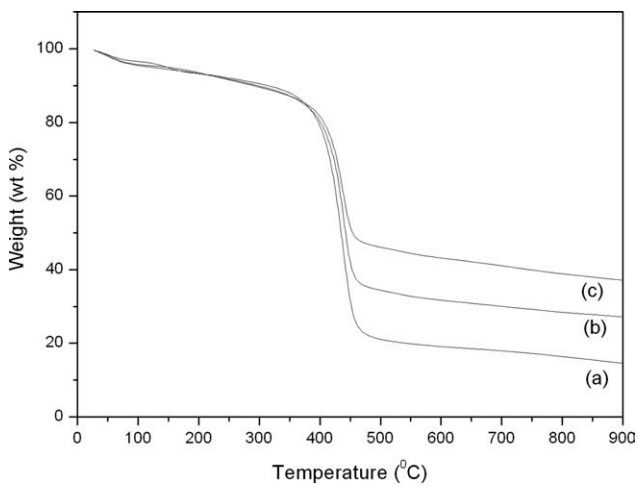

Figure 1 TG curves of (a) SiO_2/PMAA, (b) SiO_2/PMAA/PPy (pyrrole: 20 μL), and (c) SiO_2/PMAA/PPy (pyrrole: 40 μL).

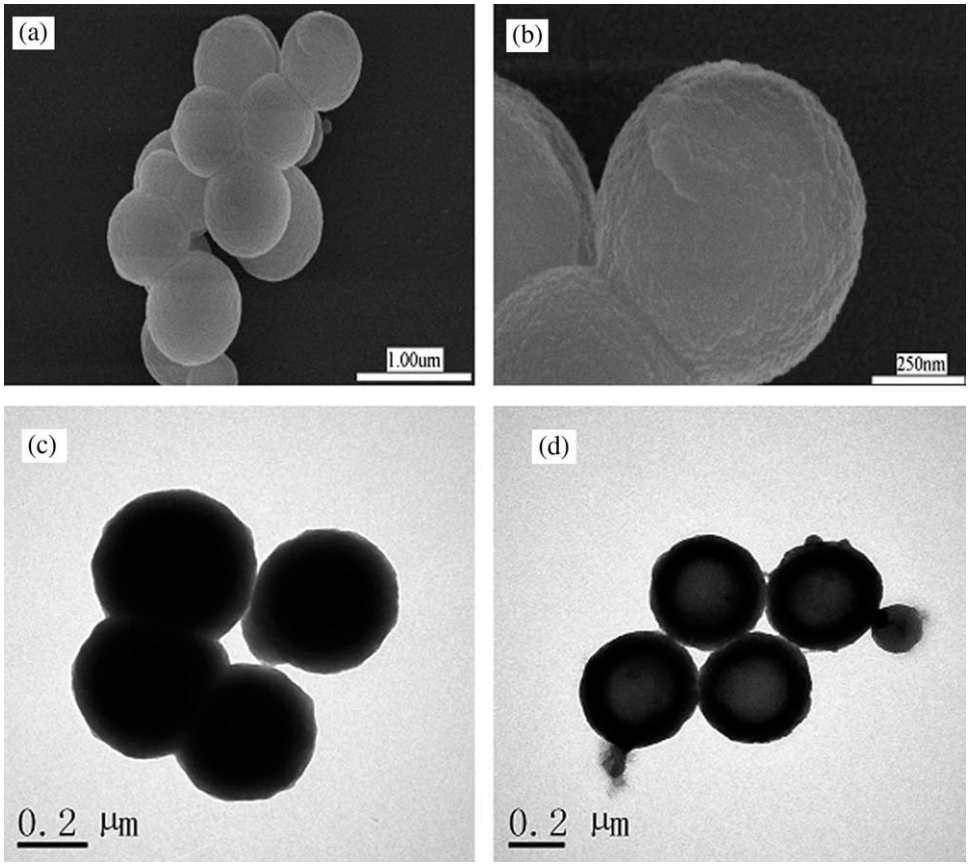

Figure 2 SEM images of SiO_2/PMAA nanocomposites: (a) low resolution, (b) higher resolution; TEM images of (c) SiO_2/PMAA nanocomposites and (d) hollow PMAA with removal the SiO_2.

initial weight loss below 200°C is due to the evaporation of moisture. The second step (200–300°C) corresponds the loss of the small molecule H_2O and CO_2 because the dehydration of PMAA to form polyanhydride.[23] The decomposed process of polyanhydride started at around 385°C, and completely ended at around 520°C. The percentages of residual SiO_2 was 17.5 wt %. The curves of SiO_2/PMAA/PPy composites with different PPy content are presented in Figure 1(b,c), respectively. It can be found that higher PPy loading resulted in larger amounts residues. Comparing curve a with curves b and c, the SiO_2/PMAA/PPy composites begin decomposing at 410°C, which are higher than that of SiO_2/PMAA composite. The result could be interpreted by the stronger hydrogen-bonding interaction between the carboxylic acid groups of PMAA and amino groups on pyrrole rings, which improved the thermodynamic stability of the resulted product.

The low-resolution SEM image of SiO_2/PMAA particles is shown in Figure 2(a). Figure 2(b) is a higher magnification SEM image obtained from a selected area of Figure 2(a), which clearly shows SiO_2/PMAA particles with relatively smooth surface and about 300 nm in diameter. Figure 2(c) provides insight into the core–shell structure of SiO_2/PMAA particle. The sharp contrast between the dark edge and the pale center in the TEM image [Fig. 2(d)] proves the hollow inside with removal of SiO_2.

Different amounts of pyrrole monomer (20 μL and 40 μL) were added into the reaction system to form SiO_2/PMAA/PPy microspheres. The morphology of resulting product could be clearly observed, and PPy shell comprised granular structures was evident [Fig. 3(a,b)], which may be due to pyrrole monomers *in situ* polymerized to form PPy nanoparticles, and these particles piled on the surface of PMMA layer.[17] Comparing Figure 2(b) to Figure 3(b), it was found that the surface of SiO_2/PMAA/PPy nanocomposites was rougher, which indicated the PMAA layer had been enwrapped by PPy. After removal of SiO_2 core, the TEM images of the responding product are shown in Figure 3(c,d). The average thickness of shell of particles in Figure 3(d) is about 80 nm, which is thicker than that of particles ($\sim$ 60 nm) in Figure 3(c). This result indicates that the composites have higher PPy loading with increase of amount of pyrrole in the reaction. The observation is also in a good agreement with TGA data.

The FTIR spectra of the SiO_2/PMAA and SiO_2/PMAA/PPy composites are shown in Figure 4. The characteristic peak at 710 cm^{-1} corresponds to the

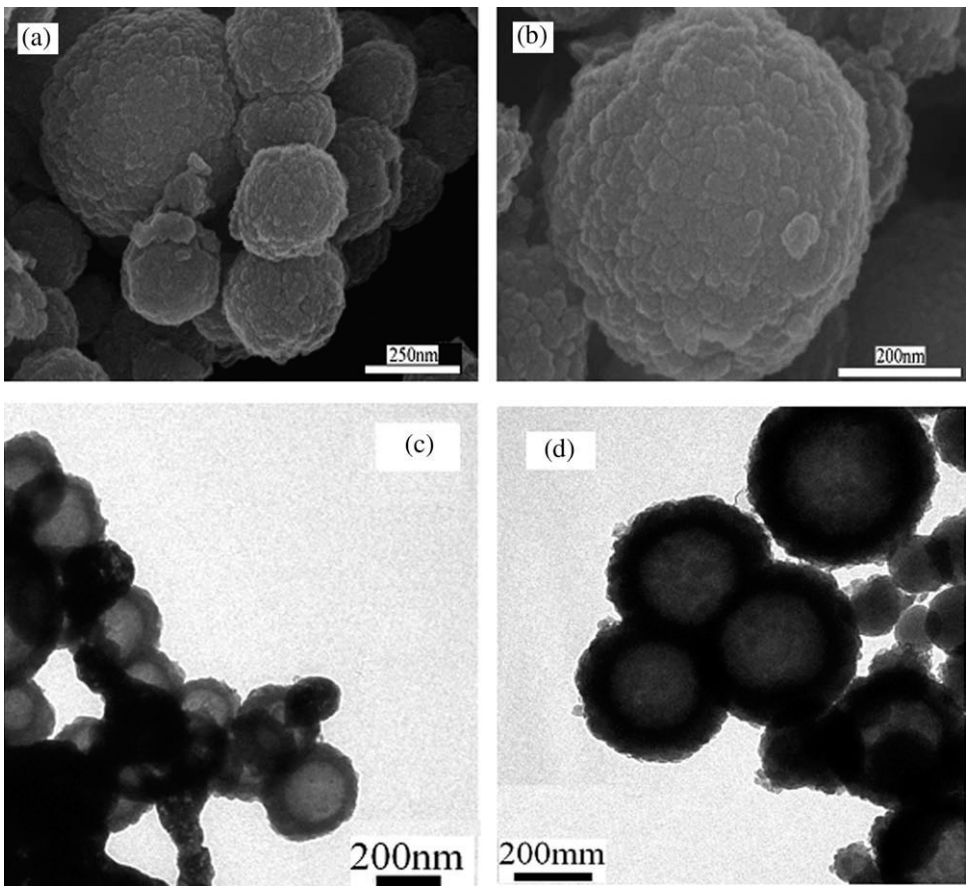

Figure 3 SEM images of SiO_2/PMAA/PPy: (a) low resolution; (b) higher resolution; TEM images of hollow structure with removal of SiO_2: (c) reaction condition: 20 μL pyrrole; (d) reaction condition: 40 μL pyrrole.

typical absorption of the phenyl group of polyDVB component. The peak at 1700 cm^{-1} in Figure 4(a) corresponding to the stretching vibration of the carbonyl group of the carboxylic acid group demonstrates that PMAA segment was incorporated onto the shell layer of the core–shell hybrids.[22] In Figure 4(b), band at 1040 cm^{-1} is assigned to a combination C—H in-plane ring bending and the deformation of the five-membered ring that contains the C=C—N deformation. The bands at 920 cm^{-1} and around 780 and 680 cm^{-1} are attributed to C=C in-plane bending of pyrrole ring and C—H out-of-plane bending in PPy, respectively.[24,25] Those data from Figure 4(b) confirm that PPy has been formed on the surface of SiO_2/PMAA.

The molecular structures of the composites were further characterized by XPS. The XPS survey spectrum of SiO_2/PMAA/PPy nanocomposites is presented in Figure 5(a), and the elements C, N, and O are detected. Figure 5(b) shows the N1s spectrum, which is deconvoluted into four peaks. The major peak at the binding energy (E_B) of 399.8 eV is attributed to the amine-like (—NH—) structure in PPy. The peak at 398.6 eV is assigned to the imine-like (=N—) nitrogen species in PPy. Two peaks at 400.8 and 402.2 eV are attributed to the positively charged nitrogen (N^+) structure.[26,27] The C1s spectrum [Fig. 5(c)] of the product can be decomposed into a series of Gaussian-Lorentzian peaks with the E_B values equal to 284.5, 286.7, and 289 eV. The main peak

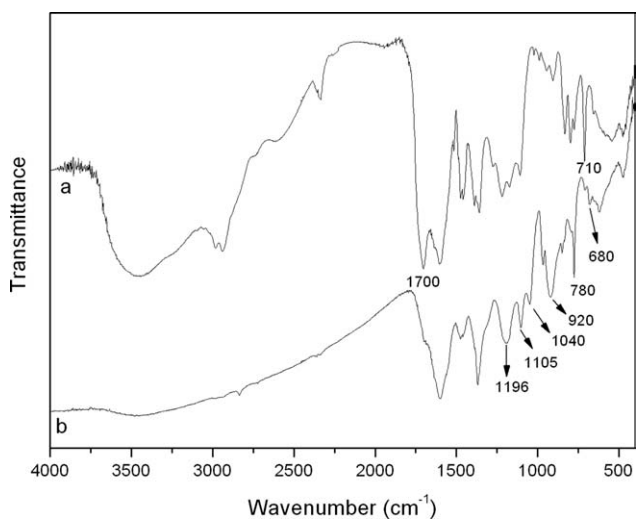

Figure 4 FTIR spectra of SiO_2/PMAA (a) and SiO_2/PMAA/PPy (b).

component at 284.5 eV is assigned to C—H, C—C, and C—N species.[28,29] The other two peaks at 286.7 and 289 eV are attributed to oxidized carbon species (C—O and O=C—O, respectively) characteristic to the presence of acetate charge.[30]

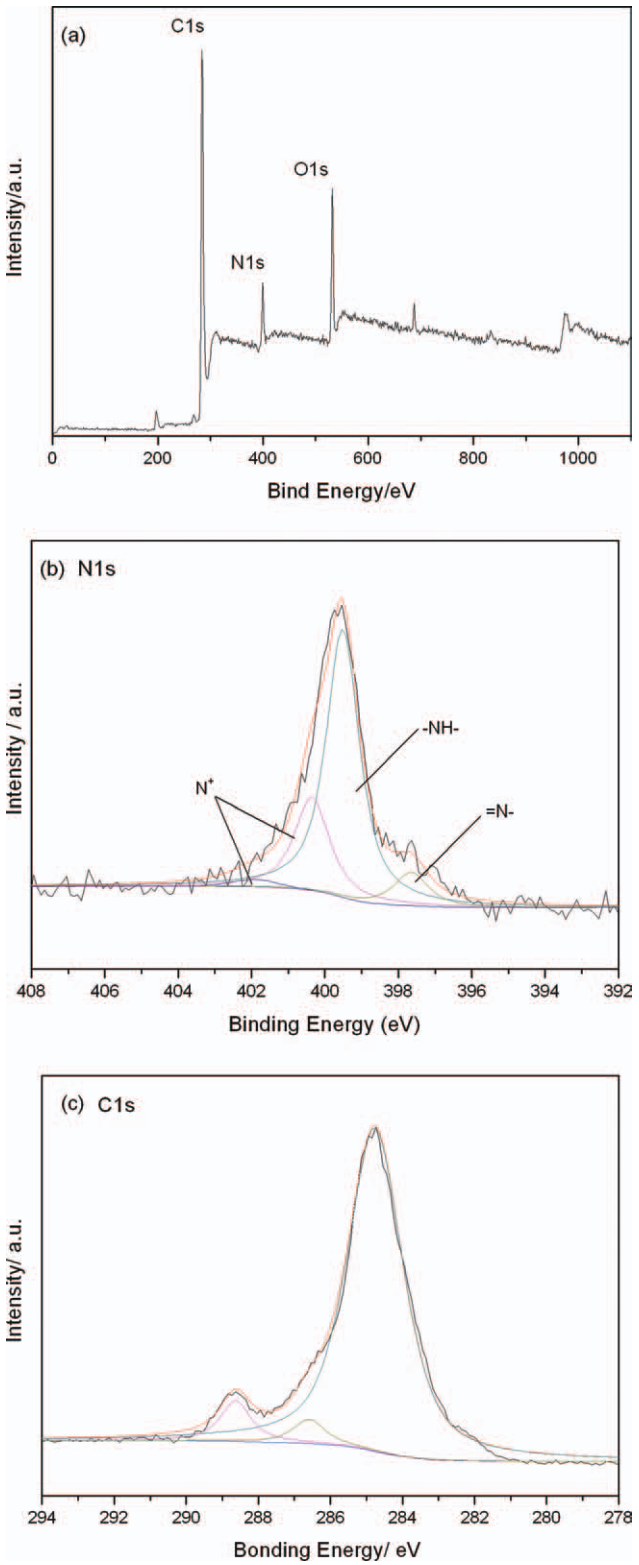

Figure 5 XPS spectra (a) survey spectra, (b) N1s, and (c) C1s. [Color figure can be viewed in the online issue, which is available at wileyonlinelibrary.com.]

TABLE I
The Conductivities of the Relevant Composites

Sample code	Conductivity of composites (S cm^{-1})	Conductivity after SiO_2 etched (S cm^{-1})
SiO_2/PPy[a]	3.7×10^{-3}	8.1×10^{-2}
SiO_2/PMAA/PPy[b]	0.38	1.2
SiO_2/PMAA/PPy[c]	0.51	1.7

[a] The SiO_2/PPy composite (see Supporting Information).
[b] Pyrrole monomer 20 μL.
[c] Pyrrole monomer 40 μL.

To investigate the influence of PMAA on the conductivity of PPy, a SiO_2/PPy composite was also prepared (see Supporting Information). These samples were pressed into disks at room temperature, and the conductivities of the samples were determined using standard four-point probe techniques. Conductivities of the relevant composites were listed on the Table I. From those data, it is found that the conductivity SiO_2/PMAA/PPy composite is much higher than that of SiO_2/PPy composite, which confirms that PMAA has a doping action on PPy. After SiO_2 core was etched, the conductivities of PPy hollow spheres were efficiently improved compared with corresponding composites.

CONCLUSIONS

In conclusion, SiO_2/PMAA/PPy composites had been successfully synthesized, and PPy hollow spheres could be obtained via HF-etched method. The size of nanocomposites and shell thickness of PPy hollow spheres could be controlled by adjusting the addition volume of pyrrole monomer. The hydrogen-bonding interaction between the carboxylic acid groups of PMAA and amino groups on pyrrole rings ensured pyrrole monomer polymerize on the PMAA layer. Compared to the SiO_2/PPy composite, the PMAA as a macromolecular doping acid could improve markedly the conductivity of PPy. PMAA-modified-SiO_2 can be used as a template to fabricate other conducting polymer/SiO_2 composites and the relevant hollow microspheres.

References

1. Jiang, P.; Berton, J. F.; Colvin, V. L. Science 2001, 291, 453.
2. Khan, M. A.; Armes, S. P. Adv Mater 2000, 12, 671.
3. Khan, M. A.; Armes, S. P. Langmuir 1999, 15, 3469.
4. Wang, S. B.; Shi, G. Q. Mater Chem Phys 2007, 102, 255.
5. Wang, W. Q.; Li, W. L.; Zhang, R. F.; Wang, J. J. Synth Met 2010, 160, 2203.
6. Wang, W. Q.; Li, W. L.; Zhang, R. F.; Wang, J. J. Synth Met 2010, 160, 2255.

7. Marinakos, S. M.; Anderson, M. F.; Ryan, J. A.; Martin, L. D.; Feldheim, D. L. J Phys Chem B 2001, 105, 8872.
8. Xuan, S. H.; Fang, Q. L.; Hao, L. Y.; Jiang, W. Q.; Gong, X. L.; Hu, Y.; Chen, Z. Y. J Colloid Interface Sci 2007, 314, 502.
9. Deng, J. G.; Ding, X. B.; Zhang, W. C.; Peng, Y. X.; Wang, J. H.; Long, X. P.; Li, P.; Chan, A. S. C. Polymer 2002, 43, 2179.
10. Kim, B. J.; Oh, S. G.; Han, M. G.; Im, S. S. Polymer 2002, 43, 111.
11. Yang, X. M.; Dai, T. Y.; Wei, M.; Lu, Y. Polymer 2006, 47, 4596.
12. Han, M. G.; Foulger, S. H. Chem Commun 2004, 19, 2154.
13. Han, M. G.; Armes, S. P. J Colloid Interface Sci 2003, 262, 418.
14. Liu, X. H.; Wu, H. Y.; Ren, F. L.; Qiu, G. Z.; Tang, M. T. Mater Chem Phys 2008, 109, 5.
15. Hao, L. Y.; Zhu, C. L.; Chen, C. N.; Kang, P.; Hu, Y.; Fan, W. C.; Chen, Z. Y. Synth Met 2003, 139, 391.
16. Cho, G.; Jung, M.; Yang, H.; Lee, B.; Song, J. H. Mater Lett 2007, 61, 1086.
17. Yang, F. Y.; Chu, Y.; Ma, S. Y.; Zhang, Y. P.; Liu, J. L. J Colloid Interface Sci 2006, 301, 470.
18. Yang, Y.; Chu, Y.; Yang, F. Y.; Zhang, Y. P. Mater Chem Phys 2005, 92, 164.
19. Kim, B. J.; Oh, S. G.; Han, M. G.; Im, S. S. Polymer 2002, 3, 111.
20. Niu, Z. G.; Yang, Z. Z.; Hu, Z. B.; Lu, Y. F.; Han, C. C. Adv Funct Mater 2003, 13, 949.
21. Bourgeat-Lami, E.; Lang, J. J Colloid Interface Sci 1998, 197, 293.
22. Liu, G. Y.; Li, L. Y.; Yang, X. L.; Dai, Z. Polym Adv Technol 2008, 19, 1922.
23. Yan, S. X. Water-Soluble Polymer; Chemical Industry Press: Beijing, 1999; p 195.
24. Kofranek, M.; Kovar, T.; Karpfen, A.; Lischka, H. J Chem Phys 1992, 96, 4464.
25. Kostic, R.; Eakovic, D.; Stepanyan, S. A.; Davidova, I. E.; Gribov, L. A. J Chem Phys 1995, 102, 3104.
26. Tan, K. L.; Tan, B. T.; Kang, G. J Chem Phys 1991, 94, 5381.
27. Neoh, K. G.; Lau, K. K. S.; Wong, V. V. T.; Kang, E. T.; Tan, K. L. Chem Mater 1996, 8, 167.
28. Vasilyeva, S. V.; Vorotyntsev, M. A.; Bezverkhyy, I.; Lesniewska, E.; Heintz, O.; Chassagnon, R. J Phys Chem C 2008, 112, 19878.
29. Liang, W.; Lei, J.; Martin, C. R. Synth Met 1992, 52, 227.
30. Moulder, J. F.; Stickle, W. F.; Sobol, P. E.; Bomben, K. D. Handbook of X-Ray Photoelectron Spectroscopy; Perkin-Elmer: Eden Prairie, MN, 1992; p 119.